

This is the peer reviewed version of the following article

**Sorgonà, A., Proto, A.R., Abenavoli, L.M. et al. Spatial distribution of coarse root biomass and carbon in a high-density olive orchard: effects of mechanical harvesting methods. *Trees* 32, 919–931 (2018).**

which has been published in final doi <https://doi.org/10.1007/s00468-018-1686-z>  
(<https://link.springer.com/article/10.1007%2Fs00468-018-1686-z>)

The terms and conditions for the reuse of this version of the manuscript are specified in the publishing policy.  
For all terms of use and more information see the publisher's website

**SPATIAL DISTRIBUTION OF COARSE ROOTS BIOMASS AND CARBON IN A HIGH-DENSITY  
OLIVE ORCHARD: EFFECTS OF MECHANICAL HARVESTING METHODS.**

**<sup>a</sup>Sorgonà A., <sup>a</sup>Proto A.R., <sup>a</sup>Abenavoli L.M., <sup>b</sup>Di Iorio A.**

<sup>a</sup>Department of Agriculture, Mediterranean University of Reggio Calabria, Feo di Vito 89122, Reggio Calabria, Italy

<sup>b</sup>Department of Biotechnologies and Life Sciences, University of Insubria, Varese, Italy

**\*Corresponding author: Prof. Sorgonà A. – email: [asorgona@unirc.it](mailto:asorgona@unirc.it); phone: +39 096516914373**

45    **Abstract**

46    **Key message:** The *in situ* 3D root architecture of *Olea europea* was described by a semi-automatic 3D digitising  
47    approach, which permitted the estimation of the biomass and carbon content of coarse roots in the soil  
48    environment.

49    *Abstract* Coarse roots, the skeleton of the root system, are of primary importance for soil exploration and plant anchorage  
50    and only recently have been recognized as playing a major role in “long-term” carbon sequestration. Despite this role, the  
51    3D architecture of coarse roots represents a gap in knowledge on the biomass and carbon allocation within the root system  
52    and, consequently, below-ground carbon sequestration capacity. Using a semi-automatic 3D digitizing approach (3 Space  
53    Fastrak plus Long Ranger), the 3D distribution in the soil environment of coarse root biomass and C content and how  
54    these parameters were affected by manual and mechanical (trunk shaker) harvesting methods were quantified in a high-  
55    density olive orchard. The below-ground C content at stand level was estimated to be 11.93 Mg C ha<sup>-1</sup> and distributed at  
56    deeper soil layers (45-60 cm) in the form of 1<sup>st</sup>- and 2<sup>nd</sup>-order branching roots. The present study also revealed that the  
57    mechanical harvesting method significantly increased both the angle of growth (0° = vertically downwards) of 1<sup>st</sup>-order  
58    lateral roots and the stump biomass, but neither the biomass allocation nor the C content was increased within the first  
59    three branching orders.

60

61    **Keywords:** root architecture, olive, harvesting method, carbon sequestration

## 62    **Introduction**

63    Agricultural systems are no longer evaluated solely on the basis of the food they provide but also on their capacity to limit  
64    impacts on the environment and to provide ecosystem services such as soil and biodiversity conservation and water  
65    quality, as well as their contributions to mitigating and adapting to climate change (Smith and Olesen 2010). The  
66    agricultural strategies contributing to the mitigation of global atmospheric change rely, but not entirely, on the reduction  
67    of CO<sub>2</sub> emissions through changes in agricultural practices (Snyder et al. 2009; Smith and Olesen 2010) and on carbon  
68    sequestration in the soil as soil organic carbon (SOC) essentially via plants (De Deyn et al. 2008; Orwin et al. 2010).  
69    For this latter strategy, the role of the root system is well recognized as a first step toward storing substantial quantities  
70    of C in terms of belowground root biomass and to delivering large amounts of C to the SOC pool by fine root turnover  
71    and/or exudates (Rasse et al. 2005). In the face of this “short-term” C storage capacity, the “long-term” carbon  
72    sequestration via coarse roots (diameter >2 mm) has been recently highlighted by several experimental results. Indeed,  
73    due to pronounced secondary growth as well as to slower turnover and decomposition rates (Zhang and Wang 2015),  
74    coarse roots showed much more C content than fine roots (Sitka spruce stands: 2.9-34 and 0.6-3.4 t C ha<sup>-1</sup> for coarse and  
75    fine roots, respectively) (Black et al. 2009). Moreover, as structural axes of the root system, coarse roots can extend up  
76    to deep soil layers, which are more favourable for long-term soil C sequestration (Kell 2011, 2012). The extensive deep  
77    root system of the trees in a secondary vegetation permits higher and more permanent C stock in the soil compared to  
78    intensive fruit crops if maintained as part of the agriculture land-use system (Sommer et al. 2000); deep-rooted perennial  
79    legumes (*Astragalus adsurgens* Pall., *Medicago sativa* L. and *Lespedeza davurica* S.) used in the revegetation of damaged  
80    ecosystems significantly increase the SOC in deep soil layers (Guan et al. 2016). Hence, accurate spatial and temporal  
81    estimates of the biomass and carbon allocation towards coarse roots are critical to assessing the magnitude of carbon  
82    stores in the soils, to understanding what determines the magnitude of these stores and to exploring how these stores will  
83    respond to different external perturbations such as environmental conditions and/or anthropogenic activity.  
84    Despite their roles in long-term C sequestration, the distribution of coarse root biomass and carbon content in the soil is  
85    largely underestimated or neglected, unlike these features for fine roots, particularly for fruit crop species (Ceccon et al.  
86    2011, Turrini et al. 2017). Biomass and carbon stock in coarse roots are generally assessed at the stand level either by  
87    extracting and weighting all coarse roots located in an elementary area of the stand around each tree or from tree  
88    inventories or by allometric scaling relationships, both linear and non-linear, between the trunk diameter and the coarse  
89    root biomass of a tree (Brassard et al. 2011). These techniques are time consuming, require huge effort and destroy the  
90    3D root architecture, i.e., the explicit 3D geometric deployment of root axes, preventing the estimation of the root C  
91    spatial distribution in the soil. Since the end of the 1990s, new devices and non-destructive techniques have been  
92    developed for quantifying coarse root system architecture including root volume location technique and semi-automatic

3D digitizing approaches (3 Space Fastrak plus Long Ranger) (Danjon et al. 1999; Di Iorio et al. 2005, 2008). Although the application mainly concerns forest species, to our knowledge no study has addressed the 3D root architecture or belowground biomass and carbon stock distribution of fruit crop species.

The olive tree (*Olea europaea* L.) is one of the most important crops in the Mediterranean region, where 97% of the world's olive oil is produced (IOOC 2013). Calabria, in southern Italy, is the second region for olive production in Italy (ISTAT, 2016). The economic sustainability of olive groves necessarily implies the reduction of production costs especially those relating to manual harvesting, which accounts for approximately 40% of the total (Abenavoli and Proto 2015; Abenavoli et al. 2016). In this respect, the current trend is to use the trunk shaker, which is the mechanical harvesting method most used in fruit orchards (Torregrosa et al. 2006; Polat et al. 2007). Operating by vibration, the tree shakers must be used at the correct frequency and amplitude to avoid a drop in quality of olive oil (Castro-Garcia et al. 2015) and damage to the branches and trunk bark as observed in citrus orchards (Torregrosa et al., 2009), table olives (Castro-Garcia et al., 2015) and oil olive trees (Sola-Guirado et al. 2014; Proto and Zimballatti 2015). Although the correct frequency and amplitude to minimize trunk and branch damage are the most studied disturbing factors (Jimenez-Jimenez et al. 2015), no investigations have focused on the effects of shaker-related vibrations on the spatial distribution of coarse root biomass and carbon in the soil environment.

In this framework, the present work aimed to provide a detailed description of 1) the 3D root system architecture and the biomass and carbon content among the different coarse root orders and at different soil depths and radial distances in a high-density olive orchard, and 2) how these parameters are influenced by two different olive harvesting methods, namely, manual (Ma) and mechanical (trunk shaker) (Me) methods. The final objective is to understand the possible contribution of coarse roots to mitigating and adapting to climate change and to address the agronomical practices to retain soil carbon for healthier soils and improved orchard productivity.

114

## 115 **Materials and Methods**

### 116 *Site description and plant material*

117 The experiments were conducted in an organic olive tree orchard at Satriano, Calabria (Italy). The site is located on a southwest-facing slope (300 m altitude, 38°39' N, 16°28'E, mean slope of 20°) on a clay loam, medium calcareous soil, with pH slightly alkaline. Adult (22 years-old) olive trees (*Olea europaea* L.) obtained by grafting of Carolea cultivar onto seedling, trained to the vase system and planted at a spacing of 6 x 5 m, equal to 334 tree ha<sup>-1</sup> density, were studied. The olive trees were non-irrigated and for the other crop management practices (fertilization, tillage and crop protection), all trees were treated equally following the recommended standards for organic cultivation as indicated by EU (Reg. CE 834/07 and 889/08) and national regulations (MD 18354/2009).

124

### 125 ***Experimental treatment***

126 Two tree rows 12 m distant (spaced by an edge row) and characterized by manual and mechanical harvesting methods  
127 were chosen for the experimental plot. The rows were localized close to each other to avoid variation in soil properties.  
128 Within these rows, twelve trees were selected for evaluating the influence of the harvesting method on root architecture.  
129 The selected trees included 6 trees for manual harvesting and 6 trees for mechanical harvesting. Table 1 shows the size  
130 parameters of the trees.

131 Mechanical harvesting started when the plants were 7 years old and was routinely applied until present, i.e, for 15 years.  
132 For mechanical harvesting, a self-propelled machine (SICOM m110S, Catanzaro, Italy) was used. This trunk shaker can  
133 execute orbital and multidirectional vibrations in succession. The main characteristics of the trunk shaker were the  
134 following: an engine power of 80 kW (110 CV), four traction wheels, a very-high frequency vibrating head (2000-2200  
135 vibrations/min) and a self-braking system. Despite the weight of the trunk shaker (5800 kg), soil compaction was not  
136 considered an experimental bias because the soil within the rows of both manual and mechanical trees received the same  
137 tillage operations.

138

### 139 ***Excavation and 3D root architecture measurement***

140 The root systems of the examined olive trees were freed from soil using high-pressure air lances (Air-SPADE 2000,  
141 Chicopee, MA, USA). An Air-Spade supplied with compressed air from a standard 4.25 m<sup>3</sup> min<sup>-1</sup> road-works compressor  
142 loosened and removed soil from around the trunks with little or no damage to roots. Root systems were exposed to depths  
143 of 1 m and to distances of 1.5 m from the trunk (Fig. 1A). The volume of removed soil was not so large as to compromise  
144 the stability of the tree. The topology, i.e, the branching hierarchic structure, was coded according to the "acropetal-  
145 development approach" with the seed-origin radicle, the primary-roots (-axis) or taproot called order zero; lateral roots  
146 emerging from the taproot were called first-order roots, second-order roots originating from these first-order laterals, and  
147 so on (Zobel and Waisel 2010). For operational efficiency, this nomenclature was adapted to the examined olive root  
148 systems with the following difference: as the taproot was not retained, this term was substituted with "stump".

149 Three-dimensional position coordinates (X, Y, Z) of the stump and the different lateral root branching orders with a  
150 proximal diameter larger than 5 mm were measured *in situ* with a 3D digitizer (3 SPACE Fastrak, Polhemus Inc.,  
151 Colchester, VT) using low-frequency electromagnetic field sensing. Device characteristics were broadly explained in  
152 previous works (Danjon et al. 1999; Di Iorio et al. 2005;). Briefly, the device consists of an electronic unit, a magnetic  
153 transmitter (Long Ranger) and a small hand-held receiver positioned by the first operator at each point to be measured.  
154 The receiver measures the X, Y, Z spatial coordinates within a sphere-wide electromagnetic field with a 4 m radius around

155 the transmitter, which is sufficient for the root systems size observed in this study. The transmitter was positioned at  
156 approximately 1.5 m above the stump with the down-slope direction in the positive *X* direction.

157 The root system architecture was measured by starting from the top of the stump and following a recursive path along the  
158 branching network. Coordinates were determined for all branching points and every 10-20 cm when roots were straight  
159 or 2 cm when roots were highly bent or tapered. Additional features recorded during measurement were the occurrence  
160 of traumatic forks, here defined as multiple root axes originating from a single, lower-order severed root or killed tip. The  
161 measurement was driven by PiMgr software (Polhemus, Colchester, VT, USA). Root diameters, measured by a digital  
162 calliper, and topology were entered by the second operator on a Microsoft Excel spreadsheet. After the 3D root  
163 architecture measurement, the root systems were covered again with the original soil to reduce disturbance.

164

### 165 ***Root architecture analysis***

166 Roots were assumed to be either circular or elliptical in cross-section. The geometric mean of the maximum and minimum  
167 diameter determined the mean diameter of oval shaped roots. The output data file was analysed using AMAPmod software  
168 (Godin et al. 1997), which handles topological structure and provides 3D graphical reconstruction for data checking (Figs.  
169 1A, B). The extracted data were exported to Microsoft Excel 2010 (Microsoft Office, USA) to perform specialized  
170 processing. The distance between two corresponding measurement points was used as the segment length. The segment  
171 volume was calculated as a truncated cone from its length and proximal and distal diameters. The length or volume of a  
172 root axis was the sum of length or volume of all its segments. These computations were made with macro suitably realized  
173 with Microsoft Visual Basic 6.0.

174 In this work, the effect of treatment on symmetry of the root system was evaluated in terms of radial distribution of dry  
175 weight or centre of mass of all the first- to third-order lateral roots using a method similar to that described by Quine et  
176 al. (1991) and Nicoll and Ray (1996). To this aim, the root system was virtually located in a grid made of six 15 cm thick  
177 cylinders stump centred and stacked to 90 cm depth, roughly equalling the removed soil volume of  $\approx 7 \text{ m}^3$  (Fig. 1C).  
178 Depending on the different values of stump diameter (30 – 75 cm), cylinders were 1.15 – 1.36 m radius from the stump  
179 centre because, to allow comparison between root systems, calculations were performed at a standard distance of 1 m  
180 from the stump surface (Fig. 1C). Cylinders were divided into ten 36° wide sectors (Fig. 1D), giving 60 boxes (10 sectors  
181 x 6 cylinders) in total. Within each box, all first- to third-order lateral roots were virtually sliced and their volume was  
182 determined. The root system was aligned so that the 0-36° and 324-360° sectors coincided with the down-slope direction,  
183 and the 144-180° and 180-216° sectors coincided with the up-slope direction.

184 Another architectural trait investigated to evaluate differences in the growth response to mechanical stress due to the  
185 harvesting method was the angle of growth (AoG) for each first-, second- and third-order lateral root axis. It was defined  
186 by the angle between the gravity vector and the vector parallel to the segment and was measured at 10 cm length intervals.  
187

#### 188 ***Biomass and carbon evaluation.***

189 The root biomass was estimated by conversion using the density value empirically obtained by root core samples extracted  
190 from roots of different diameters with an increment corer 0.5 cm in diameter (Haglöf Sweden AB, Sweden,  
191 www.haglofsweden.com). In detail, the green volume of root core samples was calculated ( $\pi r^2 \times \text{length of core sample}$ ),  
192 and the dry mass was obtained after the samples were dried in an oven at 105 °C for 48 hours.

193 Carbon concentration ( $\text{g g}^{-1}$  DW) was measured on the same root core samples with a CHN-analyser (CN628, Leco  
194 Corporation, USA).

195 The carbon content at the tree level was calculated by multiplying the total root biomass (stump plus lateral roots) by the  
196 C concentration. The carbon content at the stand level ( $\text{Mg C ha}^{-1}$ ) was estimated by scaling-up the mean (6 replicates for  
197 each treatment) individual belowground carbon content by the tree density ( $334 \text{ trees ha}^{-1}$ ).  
198

#### 199 ***Statistical analysis***

200 Statistical analysis was conducted using SPSS Inc., V. 10.0, 2002 (SPSS Inc., Evanston, IL, USA) except where otherwise  
201 indicated.

202 Significant differences between harvesting methods for the aboveground parameters and biomass among the different  
203 root orders were evaluated by Student's t test at  $P < 0.05$ .

204 Within each harvesting method, the clustering tendency of the first-, second- and third-order laterals was evaluated using  
205 circular statistical methods, namely, the Hotelling's test (Fisher 1993; Mardia and Jupp, 2000) by Oriana software v. 4.02  
206 (Kovach Computing Services; Kovach 1994). Hotelling's test calculates whether the centroid of the end points of the  
207 weighted vectors differs from the origin, i.e., whether the weighted angles have a significant mean direction at the  
208 probability level of 0.05.

209 The occurrence of a preferred AoG for the first- to third-order lateral roots at different distances from the stump junction  
210 was evaluated using Rayleigh's Uniformity Test. The null hypothesis is that the data are uniformly distributed. The Z  
211 value is calculated as  $Z = nr^2$ , where  $n$  is the number of observations and  $r$  is the length of the mean vector. A greater  
212 mean vector length (and the resulting larger Z value) means a greater concentration of data around the mean and thus less  
213 likelihood of the data being uniformly distributed.



214 In the case of significant mean direction, differences between the mean AoG of the two harvesting methods were evaluated  
 215 by the Watson-Williams F-Test. This test basically proceeds by comparing the lengths of the mean vectors for each sample  
 216 with that of the pooled data (Gran mean vector). The resulting F statistic is the same as Fisher's variance ratio statistic  
 217 which is commonly used in linear statistics. Means were considered significantly different at  $P$  values less than 0.05.  
 218 Differences in the various components of below-ground biomass between the two harvesting methods were tested by  
 219 analysis of variance. Linear or non-linear regression analyses were performed to test the effects of depth of emission and  
 220 of the AoG of the different root branching orders.

221

## 222 **Results**

### 223 ***3D root architecture, biomass distribution between stump and coarse root branching orders, and root C content of*** 224 ***olive trees.***

225 The 3D root architecture of the mature olive trees was digitalized "*in situ*" after removing the upper soil layers and  
 226 reconstructed by AMAPmod software (compare Figs. 1C, 1D).

227 The stump biomass was on average  $70.63 \pm 20.19$  kg DW whereas the total coarse lateral root biomass was  $2.89 \pm 0.33$   
 228 kg DW m<sup>-2</sup> (Table 2), which was unevenly allocated among the first three investigated root branching orders (insert box  
 229 in Fig. 2A). In particular, for the total coarse lateral root biomass, 1<sup>st</sup> branching order, the proximal diameter ranged by  
 230 25% from 6 to 14 cm (data not shown) and accounted for 80% of the total, whereas 2<sup>nd</sup> and 3<sup>rd</sup> orders accounted for 17%  
 231 and 3%, respectively (insert box in Fig. 2A; Table 2).

232 In relation to the biomass distribution of the different root branching orders in soil depth, it was observed that most of the  
 233 biomass was located in the deeper soil layers (Fig. 2A). In particular, the biomass of the 1<sup>st</sup>-branching order roots showed  
 234 a peak at 45-60 cm of soil depth, unlike the 2<sup>nd</sup> (30-45 cm) and the 3<sup>rd</sup> orders which were closer to the soil surface (0-15  
 235 cm) (Fig. 2A).

236 In relation to the biomass radial distribution of the different root branching orders in the soil environment, the three root  
 237 orders showed a well-defined pattern (Fig. 2B). In particular, coinciding at 0 degrees with the down slope direction, the  
 238 mean growth direction of the 2<sup>nd</sup> branching order pointed to the 288-324 degree sector, whereas that of the 1<sup>st</sup> and 3<sup>rd</sup>  
 239 branching orders mostly pointing to 180°, i.e., the up-slope direction, although not significantly (Hotelling's test  $P > 0.1$ )  
 240 (Fig. 2B).

241 The carbon concentration of the coarse roots resulted on average 48.9% (Table 2). Given the detailed root biomass  
 242 information, it was possible to estimate the coarse lateral root C content at the tree level ( $2.78 \pm 0.3$  kg C m<sup>-2</sup> tree<sup>-1</sup>,  
 243 inferable from Table 2). Furthermore, considering the mean stump biomass and the 334 tree ha<sup>-1</sup> density in the investigated  
 244 olive orchard, the total coarse root C stock at the stand level amounted to 11.93 Mg C ha<sup>-1</sup> (Table 2).

245

246 *Effects of harvesting methods on olive 3D root architecture*

247 The harvesting methods did not influence the aboveground parameters of olive trees, with the only exception of the DBH  
248 (Diameter at Breast Height) (Table 1), as well as the biomass allocation among the different root branching orders (Table  
249 2). In contrast, the biomass of the stump and the third-branching order were significantly ( $P<0.001$ ) higher and markedly  
250 lower, respectively, in manually harvested trees compared to the mechanically harvested trees (Table 2).

251 Differences emerged at the architectural level in terms of the spatial distribution of the root biomass in the soil  
252 environment (Figs. 3, 4). In fact, in relation to soil depth, the 1<sup>st</sup> branching order biomass showed a depth-skewed  
253 Gaussian-like pattern for both harvesting methods (Figs. 3A, 3B). Unlike the 1<sup>st</sup> root order, the biomass of the 2<sup>nd</sup> and, to  
254 a lesser extent, the 3<sup>rd</sup> branching orders of the mechanical-treated trees, but not manual ones, showed a normal-like  
255 distribution due to a higher biomass contribution within the first 45 cm of soil depth (Fig. 3B).

256 The radial distribution of the biomass of the three different root branching orders markedly differed between the two  
257 harvesting methods, though not significantly (Fig. 4). For the 1<sup>st</sup> branching order in particular, the radial distribution  
258 showed a higher clustering tendency in mechanically treated trees (Hotelling's test  $P=0.197$ ) than manually treated trees  
259 (Hotelling's test  $P=0.735$ ); and the growth direction pointed towards the 144-216-degree sectors (Fig. 4), i.e., those  
260 located in the up-slope direction.

261 The AoG of the three root branching orders did not significantly change along the axis, resulting in a significant mean  
262 growth direction (Rayleigh's Uniformity Test,  $P<0.001$ ) for both manually and mechanically treated trees (Figs. 5A, 5B,  
263 5C). Comparing the two harvesting methods within each branching order, the mean AoG of the first branching order was  
264 significantly (Watson-Williams F-test,  $P<0.001$ ) wider in mechanically treated trees ( $80.02^\circ$ ) than manually treated trees  
265 ( $68.29^\circ$ ) (Fig. 5A). Conversely, no significant difference ( $P>0.1$ ) occurred for the 2<sup>nd</sup> and 3<sup>rd</sup> orders (Figs. 5B, 5C), the  
266 mean direction of which was  $\approx 77^\circ$  for all.

267 The AoG linearly decreased with soil depth independently from the position on the root axis (Fig. 6) but differently  
268 between the two harvesting methods. In fact, the regression slope was significantly steeper in mechanically treated trees  
269 only for the 2<sup>nd</sup> branching order roots ( $P=0.024$  in Table 3; Sokal and Rohlf 1995), highlighting a pronounced decrease  
270 from the surface to the deeper soil layer. Conversely, no difference occurred for the 1<sup>st</sup> ( $P=0.149$ ) and the 3<sup>rd</sup> branching  
271 order ( $P=0.065$ ), although the latter partially missed the significance (Table 3). Moreover, the R-square in mechanically  
272 treated trees was slightly higher than that in manually-treated trees independent of the root branching order, in accordance  
273 with the narrower 95% confidence range.

274 The C concentration did not differ between the two harvesting methods (48.7 % and 49.1%, respectively), whereas the C  
275 content was more than 3-fold higher ( $P=0.016$ ) in manually treated trees compared to mechanically treated trees both at  
276 the tree and stand levels (Table 2).

277

## 278 Discussion

### 279 *3D root architecture in situ, biomass distribution between stump and coarse root branching orders, and root C content* 280 *of the olive trees.*

281 Using Fastrak technology and AMAPmod software, the 3D root architecture of the mature olive trees was reconstructed  
282 *in situ* for the first time (Figs. 1C, 1D). 3D root architecture digitalization *in situ* has already been performed in different  
283 species (*Quercus*: Di Iorio et al. 2005; *Pinus*: Danjon et al. 1999, 2005; *Picea*: Nicoll et al. 2006; *Spartium*: Di Iorio et  
284 al. 2008; *Zea mais*: Wu et al. 2015; *Jathropa curcas*: Valdés-Rodríguez et al. 2013) but not in fruit orchards. The *in situ*  
285 digitalization and the subsequent 3D root architecture reconstruction made it possible to non-destructively estimate 1) the  
286 biomass allocation within the root system and 2) how this root biomass was spatially distributed in the soil.

287 Within the root system, most of the biomass was allocated to the stump down to 40 cm soil depth (Table 2) in the form  
288 of new characteristic protuberances (tissue hyperplasia; electronic supplementary information 1), which usually extrude  
289 from the collar of adult trees (Fabbri et al. 2004). To our knowledge, there is no evidence in the literature for the occurrence  
290 of these protuberances at greater soil depths.

291 The observed biomass allocation pattern, characterized by more biomass in the 1<sup>st</sup> rather than in the higher branching  
292 orders (insert box in Fig. 2A), may influence the long-term carbon sequestration by the coarse roots in olive trees. In fact,  
293 larger roots feature a slower decomposition rate (Zhang and Wang 2015; Luo et al. 2016), longer life spans and greater  
294 resource conservation compared to fine roots (Eissenstat et al. 2000; Withington and Reich 2006; McCormack et al.  
295 2012). In terms of carbon stocks, for example, across a Sitka spruce (*Picea sitchensis* (Bong.) Carr.) chronosequence (9–  
296 45-years old), the C-stocks of coarse roots (2.9–34 Mg C ha<sup>-1</sup>) were significantly higher than those of fine roots (0.6–3.4  
297 Mg C ha<sup>-1</sup>) (Black et al. 2009).

298 The coarse root biomass of the examined olive trees showed a depth-oriented distribution of the 1<sup>st</sup> and, to a lesser extent,  
299 2<sup>nd</sup> branching orders (Fig. 2A), i.e., the largest coarse roots, in the soil environment. This biomass distribution pattern was  
300 in accordance with those obtained with soil coring methods by Turrini et al. (2017), Chiraz (2013) and Michelakis and  
301 Vougioucalou (1988). Furthermore, this distribution could be very important for the C stock capability of the olive  
302 orchards because deeper soil layers are considered a conservative environment with a low organic decomposition rate  
303 (Sommer et al. 2000; Schrumpf et al. 2013; Guan et al. 2016).

304 The radial distribution of the coarse root biomass showed an elongation direction preferentially oriented up-slope,  
305 although not significantly (Fig. 2B). In steep slope condition, a prevalent distribution of *Quercus sp.* thicker lateral roots  
306 in the upslope soil sector was observed (Chiatante et al. 2003, Di Iorio et al. 2005 and Danjon et al. 2008), a spatial  
307 arrangement the authors related to the mechanical stability function of coarse roots and, probably, the uneven soil water  
308 distribution around the tree due to the downward flow direction. In this study, the lack of significance in the clustering  
309 tendency particularly for the first-order lateral roots was probably due to the moderate inclination of the slope.  
310 This study also revealed that the carbon content estimated at the stand level (11.93 Mg C ha<sup>-1</sup>) is in accordance with that  
311 observed in the coarse roots of forest species estimated by the current Canada national greenhouse gas inventory (12.35  
312 Mg C ha<sup>-1</sup>, Smyth et al. 2013) and climate-derived predictions (12.20 Mg C ha<sup>-1</sup>, Reich et al. 2014) and of mature  
313 *Nothofagus antarctica* (8.2-13.5 Mg C ha<sup>-1</sup>; Peri et al. 2010).

314

#### 315 ***Effects of harvesting methods on olive 3D root architecture: biomechanics and C stock capability***

316 Depth of emission partially explains the root localization in the soil layers, as it is the direction of its elongation, i.e., the  
317 AoG, that determines the final root position in the soil environment. The trunk shaker harvesting method caused the  
318 “surfacing” of the biomass, particularly in the first branching order roots, i.e., the most important roots for tree anchorage,  
319 whereas a higher stump biomass occurred in manually harvested trees (Fig. 5).

320 It could be assumed that most of the measured first-order roots, i.e., the largest ones, were already present at the onset of  
321 the mechanical harvest, when trees were 7 years old; for example, in *Quercus cerris* (Di Iorio et al. 2007), structural roots  
322 with a proximal diameter of 8-9 cm can reach lengths greater than 1 m during the first year of growth. Therefore, the  
323 smaller range of AoG variation at a given soil depth (see the R<sup>2</sup> in Table 3) together with the significantly wider AoG of  
324 the 1<sup>st</sup> branching order roots for the mechanically harvested trees (Fig. 5) highlighted how the mechanical action  
325 constrained the morphogenesis of those roots most important for anchorage. Root system architecture, in fact, can be  
326 considered as the network of directions followed by aboveground-acting forces during their transfer to the ground (Ennos  
327 1993). Clearly, these dynamic forces stimulate acclimation processes in terms of both basal diameter and rigidity increases  
328 in those roots lying along the axis of unidirectional forces such as wind (Stokes et al. 1995; Goodman and Ennos 1998)  
329 or sloping terrain (Di Iorio et al. 2005). Recent investigations and simulations on root architectural components that best  
330 contribute to anchorage show that root secondary thickening increases anchorage strength by 58% (Yang et al 2016) and  
331 that preferential acclimation occurs in the middle of the taproot and in windward and leeward shallow roots within their  
332 zone of rapid taper (Danjon et al. 2008; Yang et al 2016), where stresses are higher. Therefore, the wider AoG measured  
333 in this study could be due to 1) the asymmetric secondary growth along the root axis and/or 2) the small displacement  
334 occurring when lateral roots were pushed and bent into the soil during trunk shaking. From a mechanical point of view,

trunk shaking differs from the unidirectional loadings characterizing the slope and wind stressors in that it combines very high periodical force with an extremely high number of individual perturbations per minute (2000-2200 vibrations/min in this study). Depending on their orientation into the soil, roots generally undergo tensile, compressive or flexural bending loads, the latter within the zone of rapid taper (Goodmann and Ennos 1998, Yang et al. 2017). The root bending stiffness and the maximum bending stress increase with the fourth and third power of the root diameter, respectively, whereas the tensile force to break roots increases only with the square of the root diameter (Yang et al. 2017 and references therein). Therefore, a small difference in root diameter, although potentially resulting in the lack of a significant difference in terms of biomass, as in the case of this study, may lead to increased flexural rather than tensile stiffness and, consequently, visible changes in its contribution to tree anchorage. The significantly wider AoG of the surface roots in the mechanically treated trees suggests a higher load in bending than in tension for these roots. Considering that a small increase in root diameter determines higher flexural rather than tensile stiffness (Goodman and Ennos 1998), the wider AoG in the mechanically treated trees could be a thigmomorphogenic acclimation (Telewski 2006) achieved through secondary growth, aimed at improving the tree anchorage for a given mass investment. Nevertheless, the reduced diameter of the stump in the mechanically harvested trees could reduce its resistance to rotation because the bending strength of a root axis is proportional to the third power of the diameter. Anyhow, the occurrence of both a symmetric radial distribution of the shallow roots and near vertically oriented lateral roots from the bottom of the stump reduces the contribution of the stump size to the tree anchorage (Ennos 1993).

In addition to biomechanical acclimation, differences in the root system architecture between the two harvesting methods could affect the C sequestration capability of the olive orchard. The mechanically treated trees characterized by both higher biomass of the lateral coarse roots in the upper soil layers and smaller sized stump exhibited lower C content (Fig. 3 and Table 2), suggesting a lower C sequestration capability than the manually treated ones. In fact, deeper soil layers are considered a conservative environment with a low organic decomposition rate and play a crucial role in sequestering C belowground (Kell 2011, 2012; Schrumpf et al. 2013). Moreover, given the lack of significant differences between the two harvesting methods for the biomass of the three examined branching orders, the stump appears to play a crucial role in carbon sequestration if olive trees are manually harvested as the biomass and, consequently, C content were lower in the mechanically harvested trees.

361

## 362 **Conclusion**

363 Through the 3D reconstruction of the root architecture of mature olive trees *in situ*, this study shows how the coarse roots, 364 i.e., the skeleton of the root system, were localized in the soil environment of a high-density orchard and how the 365 harvesting methods may partially affect their deployment. Moreover, by extrapolating the biomass and the relative C

concentration from the measured wood density, the 3D root architecture revealed spatial variation in the soil C stocks pointing out the role of the olive trees in the C sequestration capacity. Indeed, the higher root biomass (1<sup>st</sup>-and 2<sup>nd</sup>-branching order roots) preferentially located at deeper soil layers (45-60 cm), combined with the estimated belowground C stock at the stand level (11.93 Mg C ha<sup>-1</sup>), highlighted an important role of olive orchards in “long-term” carbon sequestration, as observed in other fruit orchards (Scandellari et al., 2016).

The present study also revealed that the olive harvesting methods affected the size of the stump and, to a lesser extent, the biomass distribution of the coarse lateral roots, but these methods affected neither the biomass allocation within the three branching orders nor the C content. Moreover, the root pattern along the soil layers of the mechanically treated trees was slightly different from that of the manually treated trees: the root pattern of the former exhibited a more superficial distribution but with a steeper AoG, especially for the 1<sup>st</sup> branching order, at deeper soil layers. The results of this investigation suggest that at least to some extent, this root pattern may weaken the C sequestration capacity of the mechanically treated olive trees.

#### **Author contribution statement**

The authors confirm the work contribution on our manuscript entitled “Spatial distribution of coarse roots biomass and carbon in a high-density olive orchard: effects of mechanical harvesting methods” is EQUAL and as the follows: Sorgonà A.: discussed the idea, performed the experiment, wrote the paper and prepared the manuscript for submission; Proto AR: conducted the experiment; Abenavoli L.M.: conducted the experiment; Di Iorio A.: discussed the idea, doconducted the experiment, elaborated the root architecture data and wrote the paper.

#### **Acknowledgments**

The authors are grateful to the Chiaravalloti family for the making their farm available and for their warm hospitality. The authors also thank De Rossi A., Bartolo P., and Papandrea S. for their very useful work. The authors gratefully acknowledge the two anonymous referees for their valuable comments. We are also grateful to John Levy for revising and editing the text. Research was supported by grants from Regione Calabria to Dr. Abenavoli L., project PSR 2007-2013 - Misura 124 “Sistemi innovativi per la qualità della filiera dell’olio extravergine di oliva – SIFOLIO”.

#### **Conflict of interest**

394 The authors declare that they have no conflicts of interest.

## 395    **References**

- 396    Abenavoli LM, Cuzzupoli F, Chiaravalloti V, Proto AR (2016) Traceability system of olive oil: a case study based on the  
397    performance of a new software cloud. *Agron Res* 14:1247–1256
- 398    Abenavoli LM, Proto AR (2015) Effects of the diverse olive harvesting systems on oil quality. *Agron Res* 13: 7-16
- 399    Black K, Byrne KA, Mencuccini M et al (2009) Carbon stock and stock changes across a Sitka spruce chronosequence  
400    on surface-water gley soils. *Forestry* 82:255-272
- 401    Brassard BW, Chen HYH, Bergeron Y, Pare D (2011) Coarse root biomass allometric equations for *Abies balsamea*,  
402    *Picea mariana*, *Pinus banksiana*, and *Populus tremuloides* in the boreal forest of Ontario Canada. *Biomass Bioenerg* 35:  
403    4189–4196
- 404    Castro-Garcia S, Castillo-Ruiz FJ, Jimenez-Jimenez F, Gil-Ribes JA, Blanco-Roldan GL (2015) Suitability of Spanish  
405    ‘Manzanilla’ table olive orchards for trunk shaker harvesting. *Biosystems Eng* 129:388–395
- 406    Ceccon C, Panzacchi P, Scandellari F, Prandi L, Ventura M, Russo B, Millard P, Tagliavini M (2011) Spatial and temporal  
407    effects of soil temperature and moisture and the relation to fine root density on root and soil respiration in a mature apple  
408    orchard. *Plant Soil* 342:195-206
- 409    Chiatante D, Scippa GS, Di Iorio A, Sarnataro M (2003) The influence of steep slope on root system development. *J Plant*  
410    *Growth Regul* 21:247–260
- 411    Chiraz MC (2013) Growth of Young Olive Trees: Water Requirements in Relation to Canopy and Root Development.  
412    *Am J Plant Sci* 4:1316-1344
- 413    Danjon F, Barker DH, Drexhage M, Stokes A (2008) Using three-dimensional plant root architecture in models of  
414    shallow-slope stability. *Ann Bot* 101:1281–1293
- 415    Danjon F, Fourcaud T, Bert D (2005) Root architecture and wind-firmness of mature *Pinus pinaster*. *New Phytol*  
416    168:387–400
- 417    Danjon F, Sinoquet H, Godin C, Colin F, Drexhage M (1999) Characterisation of structural tree root architecture using  
418    3D digitising and AMAPmod software. *Plant Soil* 211:241–258
- 419    De Deyn GB, Cornelissen JHC, Bardgett RD (2008) Plant functional traits and soil carbon sequestration in contrasting  
420    biomes. *Ecol Lett* 11: 516–531
- 421    Di Iorio A, Lasserre B, Petrozzi L, Scippa GS, Chiatante D (2008) Adaptive longitudinal growth of first-order lateral  
422    roots of a woody species (*Spartium junceum*) to slope and different soil conditions—upward growth of surface roots.  
423    *Environ Exp Bot* 63: 207–215
- 424    Di Iorio A, Lasserre B, Scippa GS, Chiatante D (2005) Root system architecture of *Quercus pubescens* trees growing on  
425    different sloping conditions. *Ann Bot* 95:351–361
- 426    Eissenstat DM, Wells CE, Yanai RD, Whitbeck JL (2000) Building roots in a changing environment: implications for  
427    root longevity. *New Phytol* 147:33–42
- 428    Ennos AR (1993) The scaling of root anchorage. *J Theor Biol* 161:61-75
- 429    Fisher NI (1993) Statistical analysis of circular data. Cambridge University Press, Cambridge
- 430    Godin C, Guedon Y, Costes E, Caraglio Y (1997) Measuring and analyzing plants with the AMAPmod software. In:  
431    Michalewicz, M (ed) *Advances in Computational Life Science*. Vol I: Plants to Ecosystems, CISRO, Australia, pp 63–94
- 432    Goodman AM, Ennos AR (1998) Responses of the root systems of sunflower and maize to unidirectional stem flexure.  
433    *Ann Bot-London* 82: 347–357



434 Guan XK, Turner NC, Song L, Gu YJ, Wang TC, Li FM (2016) Soil carbon sequestration by three perennial legume  
435 pastures is greater in deeper soil layers than in the surface soil. *Biogeosciences* 13:527–534

436 IOOC (2013) World table olive figures. International Olive Council. <http://www.internationaloliveoil.org>. Accessed 16  
437 February 2017

438 ISTAT, istituto Nazionale di Statistica (2016) Banche dati.  
439 [http://agri.istat.it/sag\\_is\\_pdwout/jsp/consultazioneDati.jsp](http://agri.istat.it/sag_is_pdwout/jsp/consultazioneDati.jsp) (Accessed October 2017)

440 Jimenez-Jimenez F, Blanco-Roldan GL, Castillo-Ruiz FJ, et al (2015) Table Olives Mechanical Harvesting with Trunk  
441 Shakers: Orchard Adaption and Machine Improvements. *Chem Eng Trans* 44:271–276

442 Kell DB (2011) Breeding crop plants with deep roots: their role in sustainable carbon, nutrient and water sequestration.  
443 *Ann Bot* 108:407–418

444 Kell DB (2012) Large-scale sequestration of atmospheric carbon via plant roots in natural and agricultural ecosystems:  
445 why and how. *Philos Trans R Soc Lond B Biol Sci* 367:1589–1597

446 Kovach WL (1994) Oriana for Windows, ver. 2.01. Kovach Computing Services, Pentraeth, Wales

447 Luo Y, Zhao X, Li Y, Zuo X, Lian J, Wang T (2016) Root decomposition of *Artemisia halodendron* and its effect on soil  
448 nitrogen and soil organic carbon in the Horqin Sandy Land, northeastern China. *Ecol Res* 31:535–547

449 Mardia KV, Jupp PE (2000) Directional statistics. Chichester, Wiley

450 McCormack M, Adams TS, Smithwick EAH, Eissenstat DM (2012) Predicting fine root lifespan from plant functional  
451 traits in temperate trees. *New Phytol* 195:823–831

452 Michelakis N, Vougioucalou E (1988) Water Use, Root and Top Growth of Olive Trees for Different Methods of  
453 Irrigation and Levels of Soil Water Potential. *Olea* 19:17–31

454 Nicoll BC, Berthier S, Achim A, Gouskou K, Danjon F, van Beek LPH (2006) The architecture of *Picea sitchensis*  
455 structural root systems on horizontal and sloping terrain. *Trees* 20:701–712

456 Nicoll BC, Ray D (1996) Adaptive growth of tree root systems in response to wind action and site conditions. *Tree Physiol*  
457 16:891–898

458 Orwin KH, Buckland SM, Johnson D et al (2010) Linkages of plant traits to soil properties and the functioning of  
459 temperate grassland. *J Ecol* 98:1074–1083

460 Peri PL, Gargaglione V, Pastur GM, Lencinas MV (2010) Carbon accumulation along a stand development sequence of  
461 *Nothofagus antarctica* forests across a gradient in site quality in Southern Patagonia. *For Ecol Manage* 260:229–237

462 Polat R, Gezer I, Guner M, Durson E, Erdogan D, Bilim HC (2007) Mechanical harvesting of pistachio nuts. *J Food Eng*  
463 79:1131–1135

464 Proto AR, Zimbalatti G (2015) Risk assessment of repetitive movements in olive growing: analysis of annual exposure  
465 level assessment models with the OCRA checklist. *J Agric Saf Health* 21:241–253

466 Quine CP, Burnand AC, Coutts MP, Reynard BR (1991) Effect of mounds and stumps on the root architecture of *Sitka*  
467 *spruce* on a peaty gley restocking site. *Forestry* 64:385–401

468 Rasse DP, Rumpel C, Dignac MF (2005) Is soil carbon mostly root carbon? Mechanisms for a specific stabilisation. *Plant*  
469 *Soil* 269:341–356

470 Reich PB, Luo Y, Bradford JB, Poorter H, Perry CH, Oleksyn J (2014) Temperature drives global patterns in forest  
471 biomass distribution in leaves, stems, and roots. *Proc Natl Acad Sci USA* 111:13721–13726

472 Scandellari F, Caruso G, Liguori G, Meggio F, Palese AM, Zanotelli D, Celano G, Gucci R, Inglese P, Pitacco A,  
473 Tagliavini M (2016) A survey of carbon sequestration potential of orchards and vineyards in Italy. *Eur. J. Hort. Sci* 81:  
474 106–114

475 Schrumpf M, Kaiser K, Guggenberger G, Persson T, Kögel-Knabner I, Schulze ED (2013) Storage and stability of organic  
476 carbon in soils as related to depth, occlusion within aggregates, and attachment to minerals. *Biogeosciences* 10:1675–  
477 1691

478 Smith P, Olesen JE (2010) Synergies between the mitigation of, and adaptation to, climate change in agriculture. *J Agr*  
479 *Sci* 148:543–552

480 Smyth CE, Kurz WA, Neilson ET, Stinson G (2013) National-scale estimates of forest root biomass carbon stocks and  
481 associated carbon fluxes in Canada. *Glob Biogeochem Cycles* 27:1262–1273

482 Snyder C.S., Bruulsema T.W., Jensen T.L., Fixen P.E. (2009) Review of greenhouse gas emissions from crop production  
483 systems and fertilizer management effects. *Agric Ecosyst Environ.* doi:10.1016/j.agee.2009.04.021.

484 Sokal RR, Rohlf FJ (1995) *Biometry: the principles and practice of statistics in biological research*. New York: Freeman.

485 Sola-Guirado RR, Castro-García S, Blanco-Roldán GL et al (2014). Traditional olive tree response to oil olive harvesting  
486 technologies. *Biosyst Eng* 118:186–193

487 Sommer R, Denich M, Vlek PLG (2000) Carbon storage and root penetration in deep soils under small-farmer land-use  
488 systems in the Eastern Amazon region, Brazil. *Plant Soil* 219:231–241

489 Stokes A, Fitter AH, Coutts MP (1995) Responses of young trees to wind and shading: effects on root architecture. *J Exp*  
490 *Bot* 46:1139–1146

491 Stover DB, Day FP, Butnor JR, et al (2007) Effect of elevated CO<sub>2</sub> on coarse-root biomass in Florida scrub detected by  
492 ground-penetrating radar. *Ecology* 88:1328–1334

493 Telewski FW (2006) A unified hypothesis of mechanoperception in plants. *Am J Bot* 93:1466–1476

494 Torregrosa A, Martin B, Ortiz C, Chaparro O (2006) Mechanical harvesting of processed apricots. *Appl Eng Agric*  
495 22:499–506

496 Torregrosa A, Orti E, Martin B, Gil J, Ortiz C (2009) Mechanical harvesting of oranges and mandarines in Spain. *Biosyst*  
497 *Eng* 104:18-24

498 Turrini A, Caruso G, Avio L, Gennai C, Palla M, Agnolucci M, Tomei PE, Giovannetti M, Gucci R (2017) Protective  
499 green cover enhances soil respiration and native mycorrhizal potential compared with soil tillage in a high-density olive  
500 orchard in a long term study. *Appl Soil Ecol* 116: 70-78

501 Valdés-Rodríguez OA, Sánchez-Sánchez O, Pérez-Vázquez A, Caplan JS, Danjon F (2013) *Jatropha curcas* L. Root  
502 Structure and Growth in Diverse Soils. *ScientificWorldJournal*. ID 827295. doi:10.1155/2013/827295

503 Withington J, Reich P (2006) Comparisons of structure and life span in roots and leaves among temperate trees. *Ecol*  
504 *Monogr* 76:381–397

505 Wu J, Pagès L, Wu Q, Yang B, Guo Y (2015) Three-dimensional architecture of axile roots of field-grown maize. *Plant*  
506 *Soil* 387:363–377

507 Yang M, Défossez P, Danjon F, Dupont S, Fourcaud T (2017) Which root architectural elements contribute the best to  
508 anchorage of *Pinus species*? Insights from in silico experiments. *Plant Soil* 411:275-291

509 Zhang X, Wang W (2015) The decomposition of fine and coarse roots: their global patterns and controlling factors.  
510 *Scientific Reports* doi:10.1038/srep09940

511 Zobel RW, Waisel Y (2010) A plant root system architectural taxonomy: a framework for root nomenclature. Plant  
512 Biosyst 144: 507–512

## 513 Figure captions

514 **Figure 1** 3D image reconstruction of the olive root system and sketch of the virtual grid within which all first- to third-  
 515 order lateral roots were virtually sliced and their volume determined. Comparison of the images of the olive root system  
 516 obtained (A) by camera and (B) by 3D reconstruction from digitizing using the AMAPmod software. The viewing  
 517 configuration is identical for both images, with the horizontal red axes oriented down-slope. C) Lateral view showing the  
 518 virtual 15 cm thick soil layers stacked to 90 cm depth and to 45 cm height (the latter in the case of upwardly growing  
 519 roots in the up-slope direction). D) Top view showing the ten 36° wide sectors. The X+ axis is oriented down-slope  
 520 parallel to the slope direction (0° in angular values). Calculations were performed a 1m radial distance from the bark  
 521 surface (1.2 – 1.63 m from the stump centre).

522 **Figure 2** Dry mass distribution ( $\text{kg m}^{-2}$ ) of 1<sup>st</sup>, 2<sup>nd</sup> and 3<sup>rd</sup> branching order roots of *Olea europea* (A) at different soil  
 523 depths (the insert illustrates the relative percentage (%) on the total lateral dry mass basis ) and (B) within 1 m radial  
 524 distance from the bark surface in 36° sectors. For each sector, values account for 90 cm soil depth. 0° coincides with the  
 525 down-slope direction. The black arrows from the centre indicate the mean direction (centre of mass) for each root order.  
 526 Values are the mean of 12 replicates  $\pm$  1SE

527 **Figure 3** Dry mass distribution ( $\text{kg m}^{-2}$ ) in 15-cm soil layer increments to 90-cm soil depth of the 1<sup>st</sup>, 2<sup>nd</sup> and 3<sup>rd</sup> branching  
 528 order roots of *Olea europea* trees characterized by manual (A) and mechanical (B) harvesting methods. Values are the  
 529 mean of 6 replicates  $\pm$ 1SE. \*Indicates a significant difference at  $P < 0.05$ .

530 **Figure 4** Stacked rose of dry mass distribution ( $\text{kg m}^{-2}$ ) of 1<sup>st</sup>, 2<sup>nd</sup> and 3<sup>rd</sup> branching order roots for *Olea europea* trees  
 531 characterized by manual (A) and mechanical (B) harvesting methods measured within 36° wide soil sectors. The black  
 532 arrows originating from the centre indicate the mean direction (centre of mass) for each root order. Zero degrees coincides  
 533 with the down-slope direction. Values are the mean of 6 replicates.

534 **Figure 5** Rose of frequency distribution of the angle of growth (AoG) measured at 10 cm length increments along each  
 535 root axis of the first three root branching orders [1<sup>st</sup> (A); 2<sup>nd</sup> (B); 3<sup>rd</sup> (C)] for *Olea europea* trees characterized by manual  
 536 (dark grey bar) and mechanical (light grey bar) harvesting method. The width of the wedge is 15 degree. Zero degrees  
 537 coincides with the direction of gravity.  $P$  values indicate the probability level of significant difference (Watson-Williams  
 538 F-test at  $P < 0.05$ ) between the mean AoG direction (black arrows) of the two harvesting methods.

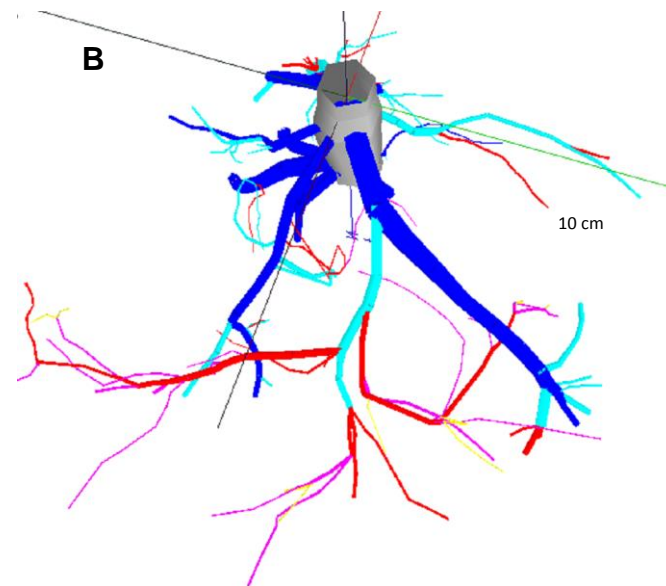
539 **Figure 6** Relationship between the Angle of growth (AoG) versus the soil depth of the first three root branching orders  
 540 [1<sup>st</sup> (top panels); 2<sup>nd</sup> (middle panels); 3<sup>rd</sup> (bottom panels)] of *Olea europea* trees characterized by manual (left column)  
 541 and mechanical (right column) harvesting methods. Each point represents the AoG value measured at 10 cm length  
 542 increments along each root axis up to a length of 150 cm. The symbol size indicates root diameter for illustrative purposes  
 543 only. The dashed lines indicate 95% confidence interval of the trendline. The regression details are reported in the Table  
 544 3.

Figure 1

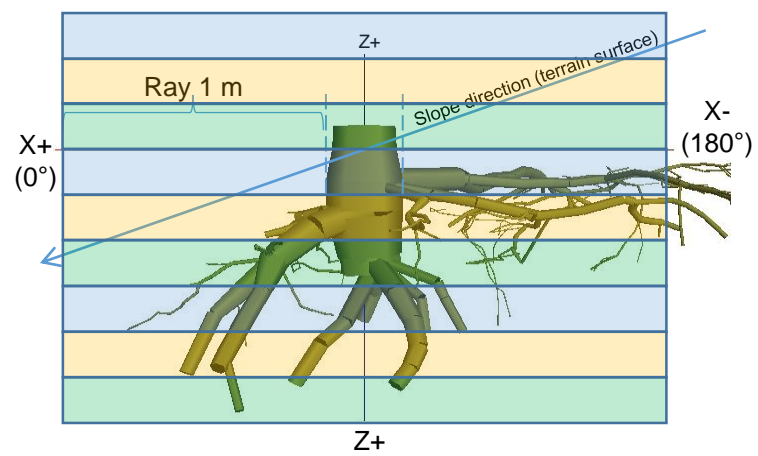
**A**



**B**



**C**



**D**

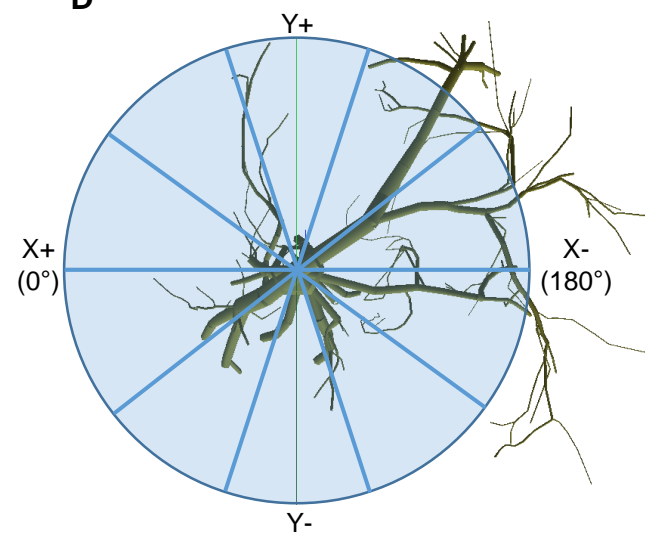


Figure 2

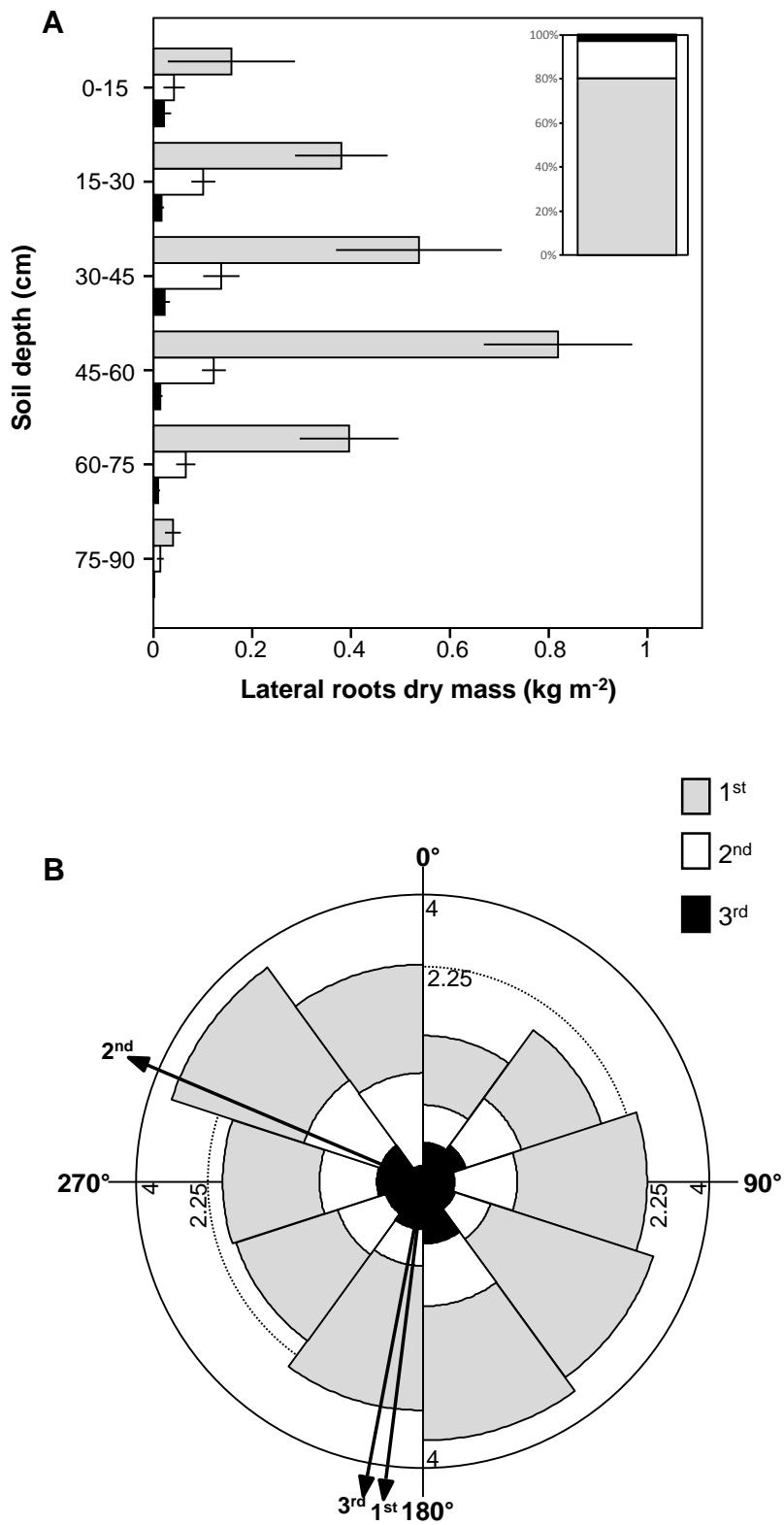


Figure 3

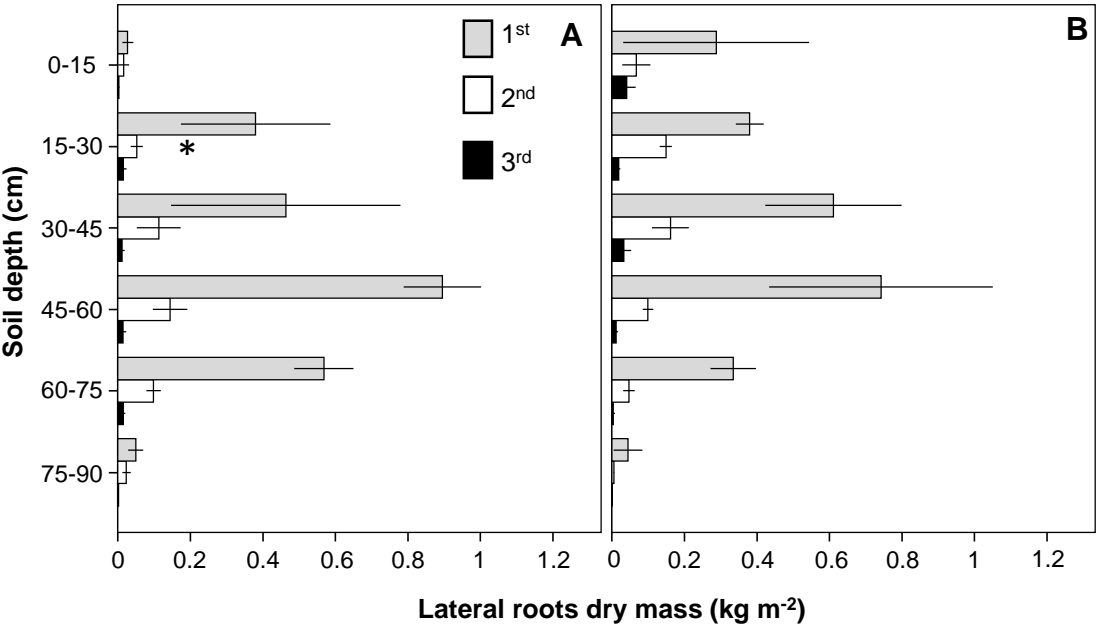


Figure 4

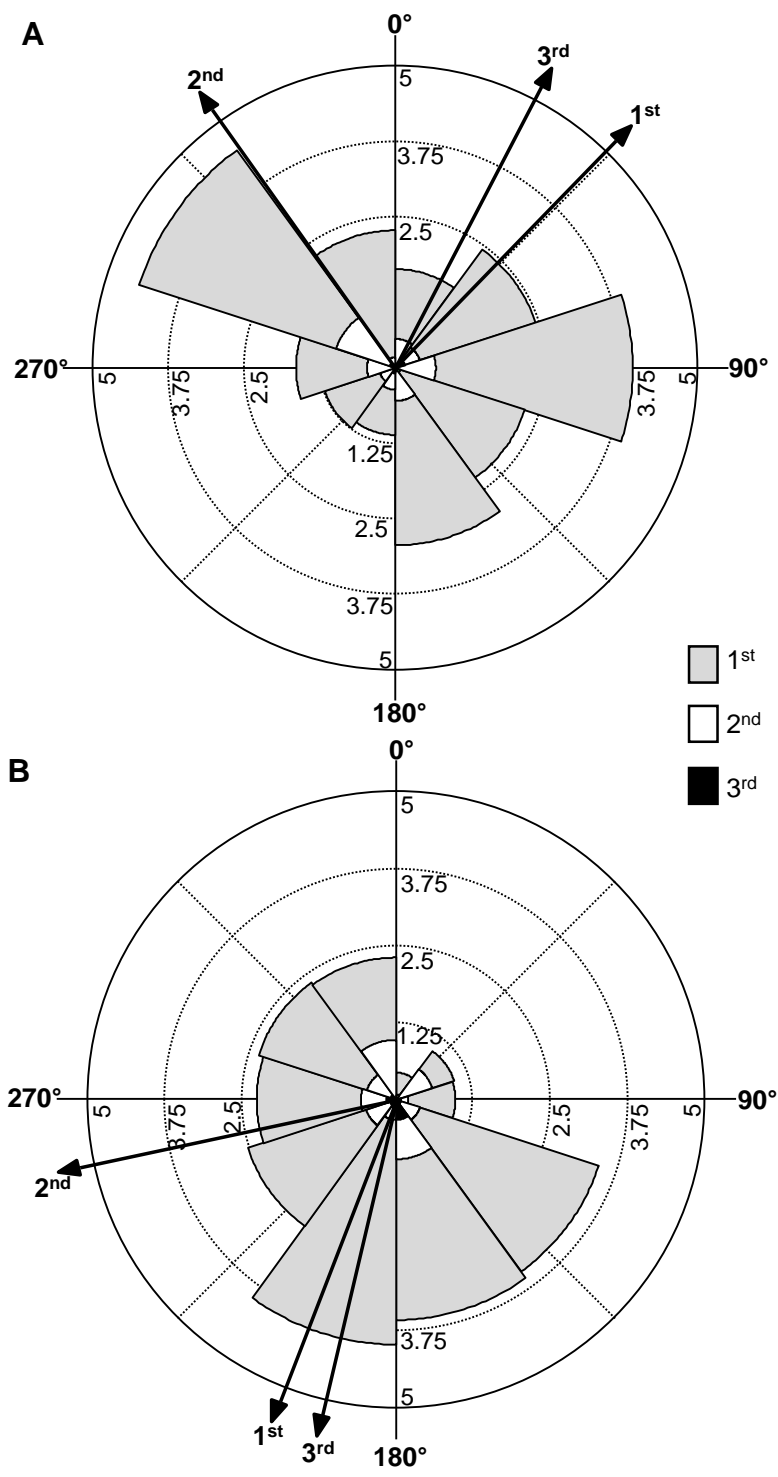




Figure 5

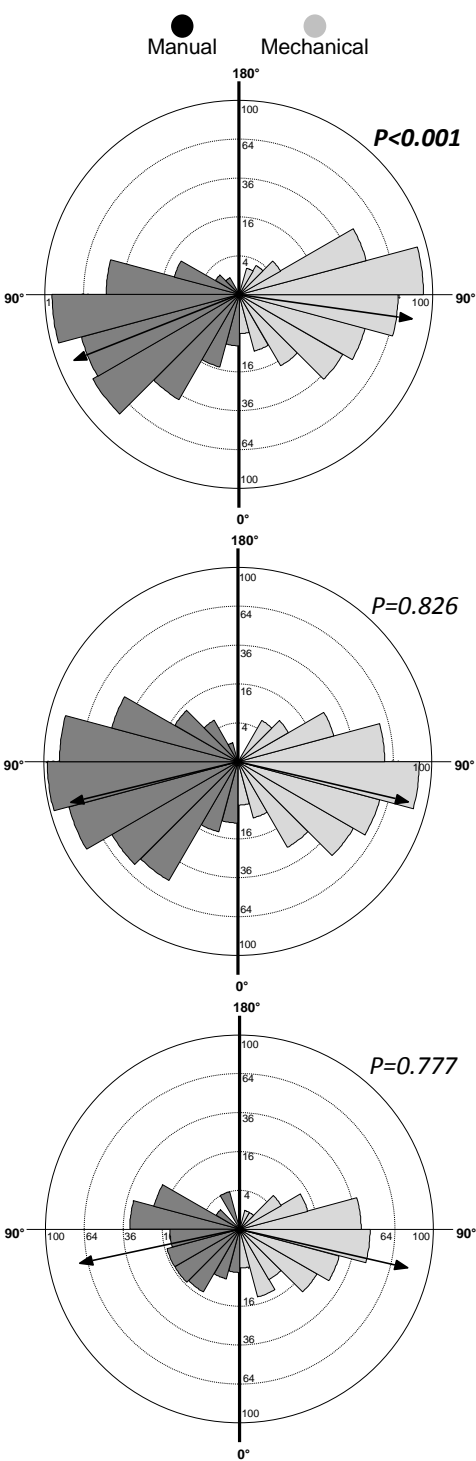
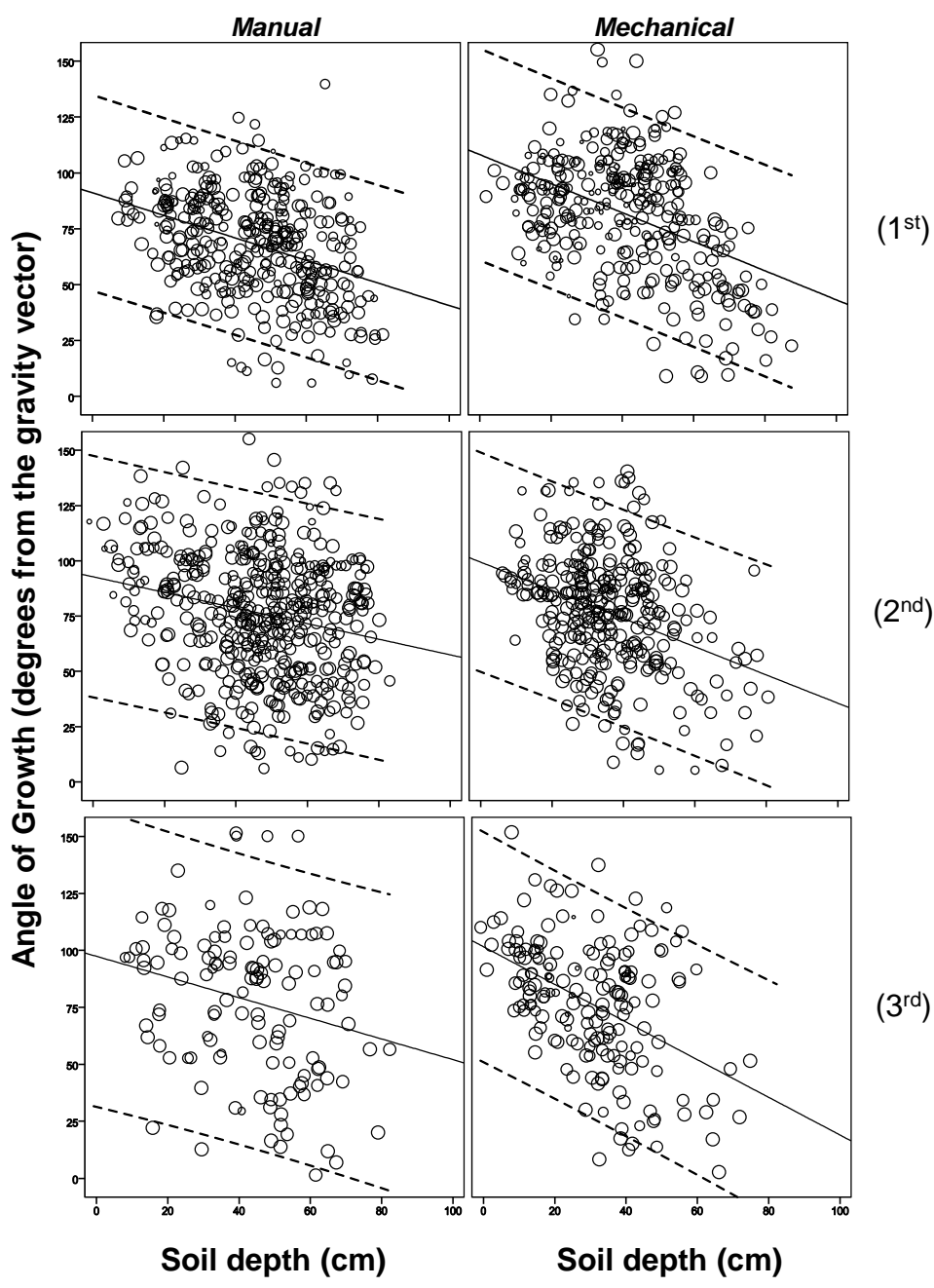


Figure 6



**Table 1** – Aboveground parameters of olive trees characterized by manual (Ma) and mechanical harvesting method (Me). DBH (Diameter at Breast Height). Different letters along the columns indicated difference at  $P<0.05$  (t-Student test) between means of 6 replicates (SE).

Treatment	DBH (m)	Plant Height (m)	Trunk Height (m)	Canopy Area (m <sup>2</sup> )
Ma	0.227 (0.012) <sup>a</sup>	4.7 (0.9) <sup>a</sup>	1.00 (0.19) <sup>a</sup>	13.1 (3.3) <sup>a</sup>
Me	0.183 (0.015) <sup>b</sup>	3.7 (0.4) <sup>a</sup>	0.87 (0.14) <sup>a</sup>	8.8 (2.4) <sup>a</sup>

**Table 2** – Dry mass at stump (kg DW) and branching order (kg DW m<sup>-2</sup>) level, carbon concentration (%) and carbon content of the whole root system at tree (Mg C tree<sup>-1</sup>) and hectare (Mg C ha<sup>-1</sup>) level for olive trees subjected to manual (Ma) and mechanical harvesting method (Me). Pooled data at orchard level is also inserted. For each parameters, different letters indicate significant differences between the two harvesting methods at 0.05 level (t-Student test). Values are the mean of 6 or 12 replicates for each harvesting method or for pooled data, respectively (SE).

	Stump (kg DW)	1 <sup>st</sup> root branching order (kg DW m <sup>-2</sup> )	2 <sup>nd</sup> root branching order (kg DW m <sup>-2</sup> )	3 <sup>rd</sup> root branching order (kg DW m <sup>-2</sup> )	Root carbon concentration (%)	Root carbon content per tree (kg C tree <sup>-1</sup> )	Root carbon content per hectare (kg C ha <sup>-1</sup> )
Pooled data	70.63 (20.19)	2.33 (0.28)	0.48 (0.06)	0.09 (0.02)	48.88 (0.30)	35.94 (9.91)	11.93 (3.31)
Ma	112.48 (14.85) <sup>a</sup>	2.39 (0.57) <sup>a</sup>	0.45 (0.12) <sup>a</sup>	0.06 (0.03) <sup>a</sup>	48.70 (0.46) <sup>a</sup>	56.18 (7.52) <sup>a</sup>	18.77 (2.51) <sup>a</sup>
Me	28.78 (8.21) <sup>b</sup>	2.28 (0.24) <sup>a</sup>	0.51 (0.06) <sup>a</sup>	0.11 (0.03) <sup>a</sup>	49.06 (0.35) <sup>a</sup>	15.54 (3.96) <sup>b</sup>	5.19 (1.32) <sup>b</sup>

**Table 3.** Linear regression equations for the relationship between the Angle of growth (AoG) versus the soil depth of different lateral root orders of *Olea europea* trees characterized by manual and mechanical harvesting method. The linear curves are shown in Figure 6. Regression slopes resulted statistically significant for all the examined equations (data not shown). *P* values indicate the probability level of significant difference ( $P<0.05$ ) between the regression slopes of the two harvesting methods (Sokal and Rohlf, 1995).

Manual Harvesting				Mechanical Harvesting			Slope comparison
	Regression equation	F	R <sup>2</sup>	Regression equation	F	R <sup>2</sup>	<i>P</i>
1 <sup>st</sup> order	y= -0.503x + 91.06	F <sub>1, 361</sub>	0.133	y= -0.65x + 108.19	F <sub>1, 326</sub>	0.188	0.149
2 <sup>nd</sup> order	y= -0.353x + 92.73	F <sub>1, 455</sub>	0.049	y= -0.637x + 99.34	F <sub>1, 327</sub>	0.115	<b>0.024</b>
3 <sup>rd</sup> order	y= -0.453x + 97.34	F <sub>1, 126</sub>	0.055	y= -0.825 + 101.52	F <sub>1, 178</sub>	0.203	0.065



**Electronic Supplementary Material 1** – Root system of a manual harvested tree. It is evident the numerous protuberances (indicated by arrows) in the large stump.